https://doi.org/10.5194/egusphere-2024-2249
Preprint. Discussion started: 22 August 2024

Brief Communication: Monitoring snow depth using small, cheap, and easy-to-deploy snow-ground interface temperature sensors

Claire L. Bachand[1], Chen Wang[2], Baptiste Dafflon[2], Lauren N. Thomas[1], Ian Shirley[2], Sarah Maebius[1], Colleen M. Iversen[3], Katrina E. Bennett[1]

[1]Earth and Environmental Sciences, Los Alamos National Laboratory, Los Alamos, NM, USA
[2]Earth and Environmental Sciences, Lawrence Berkeley National Laboratory, Berkeley, CA, USA
[3]Environmental Sciences Division and Climate Change Science Institute, Oak Ridge National Laboratory, Oak Ridge, TN, USA

Correspondence to: Claire L. Bachand (clbachand@alaska.edu)

Abstract. Temporally continuous snow depth estimates are vital for understanding changing snow patterns and impacts on permafrost in the Arctic. We train a random forest machine learning model to predict snow depth from variability in snow-ground interface temperature. The model performed well on Alaska's Seward Peninsula where it was trained, and at pan-Arctic evaluation sites (RMSE $\leq$ 0.15 m). Small temperature sensors are cheap and easy-to-deploy, so this technique enables spatially distributed and temporally continuous snowpack monitoring to an extent previously infeasible.

1 Introduction

In the Arctic, snow is an important control on permafrost, as it insulates the ground from cold winter temperatures (Shirley et al., 2022a). Changing snow patterns and associated ground insulation may accelerate permafrost thaw, leading to the release of large amounts of carbon to the atmosphere. Further, changing snow seasonality may alter the growing season and carbon uptake (Shirley et al., 2022b). Snow distribution is highly variable at fine spatial scales due to drifting snow that is affected by topography, vegetation, and wind (Bennett et al., 2022). Snow drifts form in topographic concavities (e.g., stream beds), while shrubs entrap blowing snow. These processes are poorly characterized in physics-based models (Crumley et al., 2024), and model improvements require robust and fine-scale snow depth validation. However, monitoring the spatio-temporal variability of the snowpack remains a challenge. End-of-winter snow surveys in remote, high-latitude regions (e.g., Bennett et al., 2022) are logistically difficult but capture the spatial distribution of peak snow. Automated instruments (e.g., snow sonic sensors and Snow Telemetry (SNOTEL) stations; Fleming et al., 2023) can monitor the temporal evolution of snow depth at a single point in space, but spatially distributed deployment is time consuming and expensive. Remote sensing methods to detect snow depth spatially over time are available but remain a challenge in high latitude regions (e.g., Tsang et al. 2022). To overcome these challenges, we designed a machine learning (ML) algorithm to extract snow depth from small, inexpensive temperature sensors. The model accurately estimates snow depths at sites across Alaska and the pan-Arctic. Snow characteristics have been identified using snow-ground interface temperature (T_{SG}) measurements (Lundquist and Lott, 2008;

https://doi.org/10.5194/egusphere-2024-2249
Preprint. Discussion started: 22 August 2024

Staub and Delaloye, 2017), but this is the first time, to our knowledge, that a complete time series of snow depth has been extracted from T_{SG} measurements alone.

2 Methods

We used data collected at two sites on the Seward Peninsula, Alaska (Fig. S1): 1) A 2.3 km^2 gently sloping watershed located at mile marker 27 along the Nome-Teller Highway near Nome, Alaska (hereafter Teller27) and 2) a 2.5 km^2 hillslope at mile marker 64 of the Nome-Taylor Highway (hereafter Kougarok64). The average peak snow depth from 2017-2019 at Teller27 was 0.96 m, with an average density of 0.31 g/cm^3 (Bennett et al., 2022). In 2018, snow depth was shallower at Kougarok64 than at Teller27, with an average end-of-winter depth of 0.75 m and density of 0.29 g/cm^3 (Bennett et al., 2022).

2.1 Data collection at Teller27 and Kougarok64

Collocated snow depth and T_{SG} data were collected at Teller27 and Kougarok64 over the 2021-2022 snow season via 151 paired snow and soil Distributed Temperature Profiling systems (DTPs; locations shown in Fig. S1), which measure temperatures above (snow DTP) and below (soil DTP) ground. Snow DTPs measure temperature in 5 cm increments (sensor 1-7) and 10 cm increments (sensor 8-15), to a maximum height of 1.6 m (Wang et al., 2024). When a sensor is covered by snow, high-frequency fluctuation of temperature drops dramatically, allowing snow depth to be estimated from sensor heights (Wang et al., in prep). We estimated T_{SG} from the temperature sensor closest to the snow-ground interface, which ranged from 1 cm to 5 cm *above* the ground surface. 15-minute DTP data was averaged into 4-hour intervals to match the temporal resolution of miniature temperature sensors.

Additionally, miniature iButton temperature sensors were deployed at the sites (Fig. S1). These sensors recorded T_{SG} from October 1, 2022 to September 18, 2023 in 4-hour intervals. iButtons were placed in vacuum sealed bags and distributed over variable topography and vegetation types to capture a broad range of snow conditions. We use the term "shrubs" to refer to deciduous shrubs greater than 0.4 m tall with the capacity to reach heights over 2 m (Sulman et al., 2021). Fifty-nine iButtons were placed in shrubs (89 outside of shrubs) at Teller27, while 41 were placed in shrubs (48 outside of shrubs) at Kougarok64.

2.2 Machine learning model

Using collocated DTP T_{SG} and snow depth estimates (Sect. 2.1), we developed a random forest ML model to predict snow depth from T_{SG}-derived features, which we refer to hereafter as "RF-Seward". We also tested a linear model, a simple neural network, and a Long Short Term Memory (LSTM) model. We chose a random forest as it outperformed or performed similarly to other models. A random forest is simple to design, computationally inexpensive, and easy to interpret (via feature importances). For example, permutation importance shows how random forest model performance changes when an input feature is randomly shuffled, with larger decreases in performances indicating greater feature importance (Breiman, 2001).

https://doi.org/10.5194/egusphere-2024-2249
Preprint. Discussion started: 22 August 2024

We trained RF-Seward on features derived from the 4-hour DTP T_{SG} data using hyperparameter values shown in Table S2. To temporally situate RF-Seward (i.e., incorporate information on neighboring snow conditions) and to smooth its predictions, we included daily T_{SG} standard deviations averaged over a 30-day window (length tuned using validation dataset) prior to, surrounding, and following each day as features in the model. Ultimately, RF-Seward generated a snow depth prediction for each individual day based on the following T_{SG}-derived features (listed in order of permutation feature importance): window-surrounding, window-following, window-prior, daily T_{SG} range, and daily T_{SG} maximum. We also considered T_{SG} minimum, mean, and standard deviation, but these features were highly correlated (Pearson's $r > 0.9$) with other, higher performing, features. Air temperature-derived features did not measurably improve RF-Seward and are excluded from our final model. After finalizing RF-Seward, we retrained the model on all training (96 DTPs) and validation (24 DTPs) data and evaluated its performance on the randomly selected test dataset (31 DTPs).

2.3 Model evaluation

Impact of sensor burial: Temperature sensors are often buried under a small layer of soil and vegetation to protect sensors from direct solar radiation or to monitor soil temperatures (e.g., Lundquist and Lott, 2008). To test if ML can retrieve snow depth from shallow soil temperature measurements, we trained a second ML model, which we refer to as "RF-Below". We used the same hyperparameters and features as RF-Seward, but calculated features from DTP subsurface temperature measurements recorded 1 to 5 cm *below* the ground surface. Ninety-five DTP sensors measured shallow subsurface temperatures (locations shown in Fig. S1), which we split into 76 training sensors and 19 test sensors.

Model transferability: To test model transferability, we trained RF-Seward and RF-Below at Teller27 and tested at Kougarok64, and vice versa. Further, we applied RF-Seward and RF-Below to eight evaluation datasets where T_{SG} and snow depth measurements were collocated (within approximately 5 m of each other). Sites were located in Alaska, Norway, Siberia, Colorado (CO), and New Mexico, with temperature sensors placed at the snow-ground interface or within the top 5 cm of soil (see Table S3). End-of-season snowpack bulk densities varied between sites and ranged from 0.18 g/cm^3 (Samoylov Island, Siberia, Russia) to 0.45 g/cm^3 (Senator Beck Basin, CO, USA). Vegetation also varied across sites. At Samoylov Island, the temperature sensor was deployed beneath a thick layer of tundra vegetation, while sites in New Mexico consisted of sparse grasses. Prior to this evaluation, we retrained RF-Seward and RF-Below on all available DTP data (training and test data). By training on all available data, we aim to maximize model performance by introducing the model to a broader range of snow depths and temperature responses.

Performance in deep snow: The training data available was limited to a maximum of 1.77 m due to the limited length of DTP probes, and thus RF-Seward and RF-Below cannot be used to estimate snow deeper than 1.77 m. To test if ML can be used to monitor deeper snowpacks, we trained a third ML model which we refer to as "RF-Deep". For each evaluation site, we trained

https://doi.org/10.5194/egusphere-2024-2249
Preprint. Discussion started: 22 August 2024

RF-Deep on data from all other evaluation sites (e.g., Senator Beck Basin, CO) and then ensured that snow depths above 2 m consisted of approximately 20 % of the training data.

2.4 Model application: evaluating snow-vegetation-permafrost interactions

To assess how shrubs affect snow depth and T_{SG}, we divided the iButtons deployed at Teller27 and Kougarok64 (Sect. 2.1) into two groups: within and outside of shrubs. We averaged T_{SG} measurements and RF-Seward snow depth predictions over a period corresponding to peak snow (March 20-April 9). We used the non-parametric Wilcoxon rank-sum test (Wilcoxon, 1945) to assess statistical differences in snow and T_{SG} conditions between shrubs and no-shrubs.

3 Results and discussion

RF-Seward performed well on the test dataset (R^2 = 0.87; RMSE = 0.15 m; Fig. 1a, g), but underestimated snow depths when trained at Teller27 and tested at Kougarok64 (R^2 = 0.85; RMSE = 0.17 m; Fig. 1b) and overestimated when trained at Kougarok64 and tested at Teller27 (R^2 = 0.72; RMSE = 0.23 m; Fig 1c). Differing air temperature regimes between Teller27 (warmer) and Kougarok64 (colder) may have contributed to these biases (i.e. same snow depth at the two locations corresponds to different T_{SG}). However, all RF-Seward features were derived from T_{SG} variability (not magnitudes), except for T_{SG} maximum. Excluding T_{SG} maximum from the model (not shown) did not eliminate the biases seen in Fig. 1c, d, suggesting that these errors may be tied to factors that affect T_{SG} ranges (e.g., latent heat processes). RF-Below performed worse than RF-Seward and did not transfer as well between sites (Fig. 1d – f, h, i), likely due to variability in ground insulation properties (i.e. soil type, vegetation, etc.) which confound the snow insulation effect. Further, warmer and/or wetter sites (e.g., Teller27) undergo more freezing and thawing than colder and/or dryer sites (e.g., Kougarok64), producing zero curtain periods where the key snow depth predictor (temperature variability) flattens at 0°C (Staub and Delaloye, 2017).

https://doi.org/10.5194/egusphere-2024-2249
Preprint. Discussion started: 22 August 2024

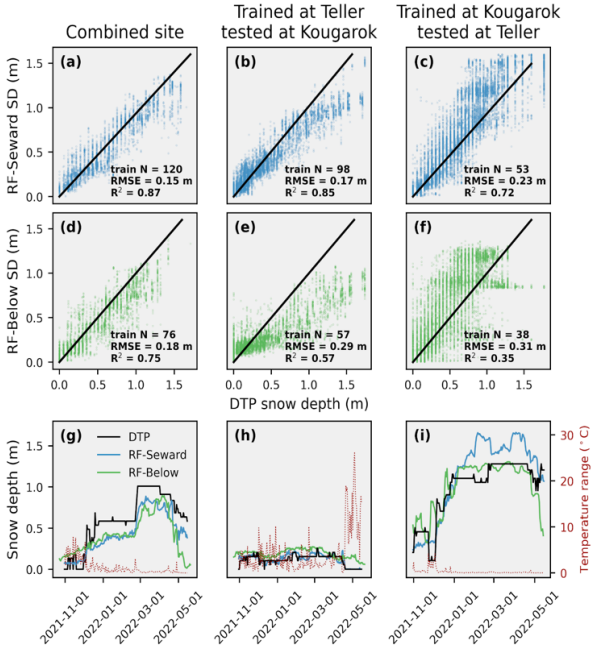

Figure 1. Performance of RF-Seward a) evaluated using test data, b) when trained at Teller27 and tested at Kougarok64, and c) visa versa. d-f) Same as a-c but for RF-Below. Time series plots of DTP snow depth data vs. ML estimates when g) trained at both sites, h) trained at Teller2, and i) trained at Kougarok64. The dotted red line shows daily temperature range, with narrower temperature ranges occurring under deeper snow cover.

RF-Seward performed well at the two sites where T_{SG} data were available in the Arctic: Bayelva station in Norway (RMSE = 0.15 m; Fig. 2a) and Imnavait Creek, on Alaska's north slope (RMSE = 0.08 m; Fig. 2b), indicating that the model may be transferable to other pan-Arctic locations. Additionally, we tested RF-Seward and RF-Below at four sites in the Arctic where temperature was recorded *below* the ground surface. At Samoylov Island (Fig. 2e), sensors were placed below an insulating layer of wet tundra vegetation, which caused RF-Seward to overpredict snow depth (mean bias = 0.40 m). RF-Below decreased overestimations at Samoylov Island (mean bias = 0.14 m) and at other sites in Alaska (Fig. 2 c,d,f). RF-Below performed best at Council, likely because vegetation at these sites is most similar to vegetation at the training study sites.

In New Mexico, paired iButtons recorded *above* and *below* ground temperature data at two sites (A and B). Predictions from iButtons placed *above* the ground surface were averaged into a single RF-Seward estimate, while predictions from iButtons placed *below* the ground surface were averaged into a single RF-Below estimate. At Site B, RF-Seward and RF-Below underpredicted peak snow by about 0.07 m (Fig. 2g). RF-Seward performed better at Site A (observed peak snow = 0.18 m; predicted = 0.16 m), although RF-Below still underpredicted by 0.10 m, possibly because the model expected insulating tundra vegetation. Both models performed poorly when applied in the wrong context (i.e. RF-Seward overpredicted peak snow by 13 cm when applied to *below* ground data; RF-Below underpredicted peak snow by 16 cm when applied to *above* ground data), indicating that excess insulation from a thin layer of soil or vegetation will be confused for snow.

https://doi.org/10.5194/egusphere-2024-2249
Preprint. Discussion started: 22 August 2024

Performance at the New Mexico sites fell within RF-Seward and RF-Below's typical ranges, despite the higher end-of-season bulk density compared to Arctic snow (~ 0.4 g/cm^3 vs. 0.3 g/cm^3). One *above* ground iButton erroneously showed delayed snowmelt due to a prolonged zero-curtain period, possibly caused by water pooling and freezing on top of the iButton's vacuum-sealed bag. Zero curtain periods were also observed in the *below* ground temperature data during snow-free periods of the winter, indicating the repetitive freezing and thawing of the soils. During these periods, T_{SG} remained static, causing RF-Below to erroneously predict the presence of snow (e.g. early accumulation in Fig. 2g). These results suggest that RF-Below will perform poorly for warm, ephemeral snowpacks, which are expected to become more common as the climate warms (Wieder et al., 2022). Zero curtain periods at the snow-ground interface can be triggered by rain-on-snow (ROS) as water percolates through the snowpack and freezes at the ground surface (Staub and Delaloye, 2017). In New Mexico, ROS events occurred from January 21 – 25, 2024, leading to erroneous increases in ML snow depth predictions.

Below ground temperature data was recorded at Grand Mesa, CO (Fig. 2h), while T_{SG} was recorded at two sites in Senator Beck Basin, CO (Fig. 2i-j). These sites accumulated more snow (up to 2.85 m) than the sites where RF-Seward was trained (maximum depth = 1.77 m), resulting in underpredictions of deep snow at these sites (Fig. 2h-j). RF-Deep predicted deeper snow depths than RF-Seward, although predictions still leveled off prematurely for some years (e.g., 2008 and 2009 in Senator Beck 2, Fig. 2j). RF-Deep also appeared visually noisy compared to RF-Seward, possibly due to the smaller training dataset and lower quality training data (i.e., temperature and snow depth measurements were not perfectly co-located). RF-Deep's poor performance indicates that at a certain depth, T_{SG} may be dampened to the extent that the ML model can no longer accurately predict snow depth. Past research has shown that snow depths greater than 1 m can completely insulate the ground, although even snowpacks deeper than 4 m are not always fully insulating (Staub and Delaloye, 2017, their Fig. 5). Because of this, it is likely that deep snow decreases the predictive value of T_{SG} measurements, which will have a minimal effect on understanding soil temperature but could cause major errors when estimating water availability from snow depth predictions.

https://doi.org/10.5194/egusphere-2024-2249
Preprint. Discussion started: 22 August 2024

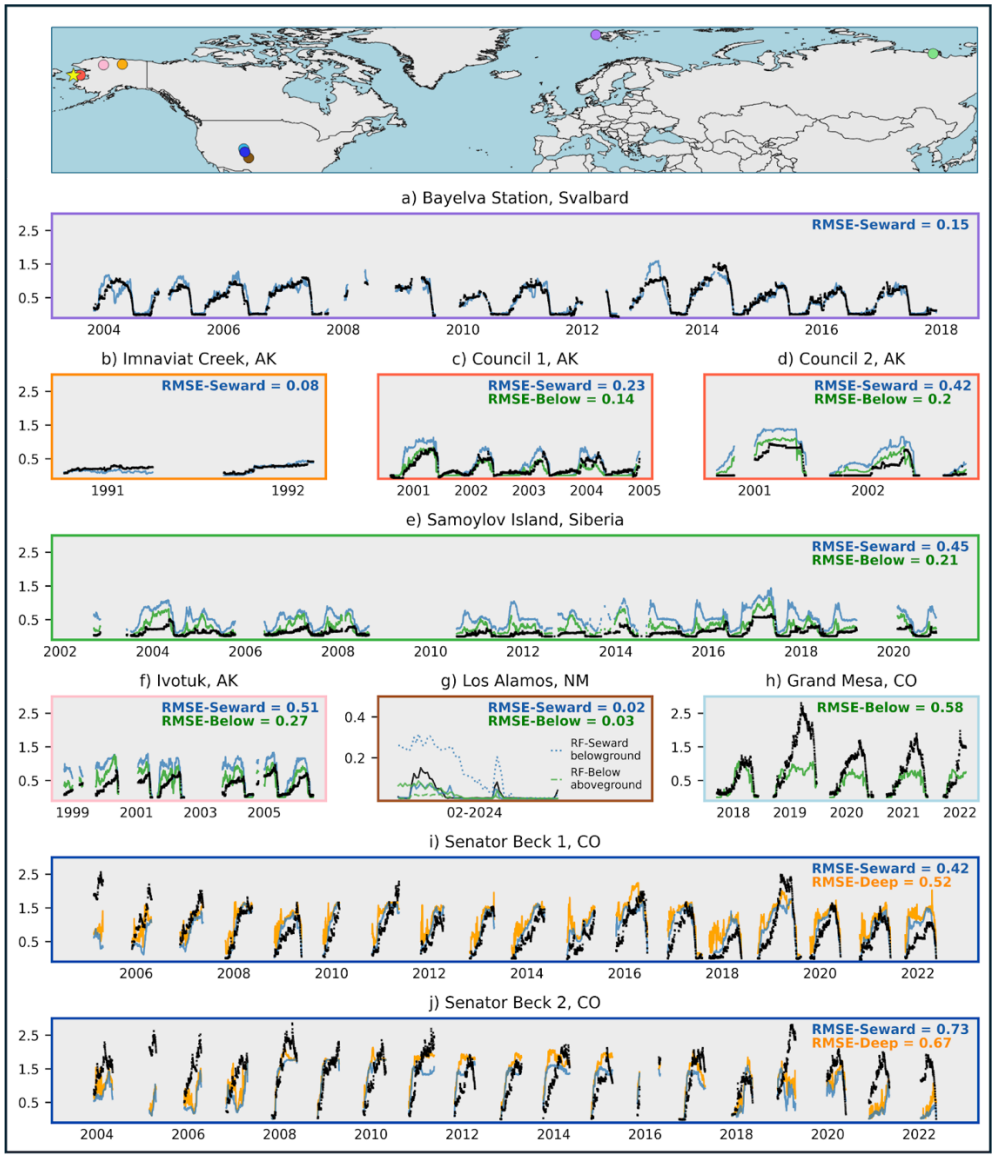

Figure 2. ML performance at sites in Svalbard (Norway), Alaska (USA), Siberia (Russia), New Mexico (USA), and CO (USA). Locations are shown on a map, with the yellow star indicating the Seward Peninsula of Alaska, where RF-Seward was trained. The color of map markers corresponds to evaluation panel outlines. f) Note adjusted color bar for Los Alamos, New Mexico. For this site, we also show RF-Seward and RF-Below predictions when RF-Below was applied aboveground and RF-Seward was applied belowground (dotted lines).

Model application: Shrubs can entrain blowing snow, resulting in snow drifts (Bennett et al., 2022). Averaged from March 20th-April 9th, the ML model estimated 33.3 cm more snow for iButtons deployed in shrubs than outside of shrubs ($p < 0.001$). This result may be biased low as RF-Seward rarely predicted more than 1.5 m of snow due to training data limitations.

https://doi.org/10.5194/egusphere-2024-2249
Preprint. Discussion started: 22 August 2024

T_{SG} averaged from March 20th to April 9th was 1.65 °C warmer in shrubs than outside of shrubs ($p < 0.001$). This suggests that Arctic shrubification (Mekonnen et al., 2021) may increase snow depths, insulate the subsurface in winter, and accelerate permafrost thaw. Topographic and landscape characteristics can drive the formation of deep snow drifts even without the presence of shrubs (Parr et al., 2020). The iButton with the third highest snow depth prediction averaged from March 20th to April 9th (1.46 m) was placed in short grasses adjacent to a stream bed, which likely experienced snow drifting due to topographic concavity (Parr et al., 2020). Similarly, the iButton with the fourth highest snow depth prediction (1.45 m) was placed near the edge of dense shrubs, where snow may have also accumulated (Currier and Lundquist, 2018).

4 Conclusions

We trained a ML model to predict snow depth from variability in snow-ground interface temperature. The model performed well on the test dataset and at two Arctic evaluation sites (RMSE <= 0.15 m). Small temperature sensors are cheap and easy-to-deploy, so this technique enables spatially distributed and temporally continuous snowpack monitoring to an extent previously infeasible. While the model generally performed well, rain-on-snow events and zero curtain periods cause the model to erroneously predict snow accumulation events. Additional co-located T_{SG} and snow depth observations could be used to retrain the ML model and enhance its transferability. For optimal performance, the model should be applied to temperatures recorded at the snow-ground interface. Predictions made using temperatures recorded *below* the ground surface were impacted by varying soil types, vegetation properties, and latent heat processes. Using ML predictions, we found that snow at Teller27 and Kougarok64 was significantly deeper in shrubs than outside of shrubs ($p < 0.001$), and that T_{SG} averaged from March 20th to April 9th was on average 1.58 °C warmer within shrubs ($p < 0.001$). Future research should focus on developing this technique for locations where peak snow depths exceed 1.5 m (e.g., CO), as these regions are crucial for water security across the world. The models developed in this study failed to accurately predict deep snow, and whether this ML technique can perform well under deep snow given a higher quality training dataset requires more investigation. Similarly, how varying end-of-season snowpack bulk densities affect model results remains unclear. The sites examined here typically experienced frozen soil prior to snowmelt, and therefore, how unfrozen soils affect ML predictions should be explored.

https://doi.org/10.5194/egusphere-2024-2249
Preprint. Discussion started: 22 August 2024

Code/Data Availability: Snow depth predictions and machine learning model code are available on the Environmental System Science Data Infrastructure for a Virtual Ecosystem (ESS-DIVE) data portal (https://doi.org/10.15485/2371854). The data package includes a *.csv file of RF-Seward and RF-Below predictions at sites in Alaska, Norway, Siberia, New Mexico, and Colorado. The code package includes a *.joblib file of the trained random forest models, which can be downloaded and directly applied to new datasets. Example workflows for cleaning data inputs, training machine learning models, and making predictions are also included in a *ipynb file. iButton temperature measurements at Teller27 and Kougarok64 (https://doi.org/10.15485/2319246) and at the Los Alamos, NM study sites (https://data.ess-dive.lbl.gov/view/doi:10.15485/2338028) are available on ESS-DIVE.

Author contributions: CLB wrote the manuscript draft, developed random forest methodology, and performed analysis; CW developed methodology to estimate snow depth using DTPs and curated data; BD, CW and IS led the DTP deployment, data collection and analysis; LNT led iButton data collection campaigns in Los Alamos, NM; SM developed LSTM methodology; CMI acquired funding and is the PI of the NGEE Arctic project; KEB developed the data collection study at Teller27 and Kougarok64, supervised research, contributed original text, and is the Institutional Lead of the NGEE Arctic project at LANL; all authors reviewed and edited the manuscript.

Competing interests: The authors declare that they have no conflict of interest.

Acknowledgements : We gratefully acknowledge Mary's Igloo (Qawiaraq in Iñupiaq), Sitnasuak, and the Council Native Corporation, for guidance and for allowing us to conduct our research on their traditional lands. The authors gratefully acknowledge the contributions of Shannon Dillard, Ryan Crumley, Eve Gasarch, Evan Thaler, Jerome Quintana, Kenneth Waight, Stijn Wielandt, John Lamb, Sylvain Fiolleau, Sebastian Uhlemann and Craig Ulrich for assisting in data collection at the Teller27, Kougarok64, and Los Alamos study sites. We thank Mia Mitchell for her assistance with Fig. 1. Further, we thank Julia Boike and Mathew Sturm for providing insight and data sources as we developed this machine learning approach.

Financial Support: The Next Generation Ecosystem Experiment (NGEE) Arctic project is supported by the Office of Biological and Environmental Research in the U.S. Department of Energy's Office of Science.

https://doi.org/10.5194/egusphere-2024-2249
Preprint. Discussion started: 22 August 2024

References

Bennett, K. E., Miller, G., Busey, R., Chen, M., Lathrop, E. R., Dann, J. B., Nutt, M., Crumley, R., Dillard, S. L., Dafflon, B., Kumar, J., Bolton, W. R., Wilson, C. J., Iversen, C. M., and Wullschleger, S. D.: Spatial patterns of snow distribution in the sub-Arctic, The Cryosphere, 16, 3269–3293, https://doi.org/10.5194/tc-16-3269-2022, 2022.

Boike, J., Juszak, I., Lange, S., Chadburn, S., Burke, E., Overduin, P. P., Roth, K., Ippisch, O., Bornemann, N., Stern, L., Gouttevin, I., Hauber, E., and Westermann, S.: A 20-year record (1998–2017) of permafrost, active layer and meteorological conditions at a high Arctic permafrost research site (Bayelva, Spitsbergen), Earth Syst. Sci. Data, 10, 355–390, https://doi.org/10.5194/essd-10-355-2018, 2018.

Boike, J., Nitzbon, J., Anders, K., Grigoriev, M., Bolshiyanov, D., Langer, M., Lange, S., Bornemann, N., Morgenstern, A., Schreiber, P., Wille, C., Chadburn, S., Gouttevin, I., Burke, E., and Kutzbach, L.: A 16-year record (2002–2017) of permafrost, active-layer, and meteorological conditions at the Samoylov Island Arctic permafrost research site, Lena River delta, northern Siberia: an opportunity to validate remote-sensing data and land surface, snow, and permafrost models, Earth Syst. Sci. Data, 11, 261–299, https://doi.org/10.5194/essd-11-261-2019, 2019.

Breiman, L.: Random Forests, Mach. Learn., 45, 5–32, https://doi.org/10.1023/A:1010933404324, 2001.

Center for Snow and Avalanche Studies: Archival Data from Senator Beck Basin Study Area, https://snowstudies.org/archived-data/, 2012.

Crumley, R., Bachand, C., and Bennett, K. E.: Snow distribution patterns revisited: A physics-based and machine learning hybrid approach to snow distribution mapping in the sub-Arctic, Water Resour. Res., 2024.

Currier, W. R. and Lundquist, J. D.: Snow Depth Variability at the Forest Edge in Multiple Climates in the Western United States, Water Resour. Res., 54, 8756–8773, https://doi.org/10.1029/2018WR022553, 2018.

Fleming, S. W., Zukiewicz, L., Strobel, M. L., Hofman, H., and Goodbody, A. G.: SNO^{TEL}, the Soil Climate Analysis Network, and water supply forecasting at the Natural Resources Conservation Service: Past, present, and future, JAWRA J. Am. Water Resour. Assoc., 59, 585–599, https://doi.org/10.1111/1752-1688.13104, 2023.

Hinzman, L. D., Kane, D. L., and Goering, D. J.: Meteorological, Radiation, Soil, and Snow Data from Alaska Sites, 1998-2008, https://doi.org/10.5065/D6G44NFV, 2016.

Houser, P., Rudisill, W., Johnston, J., Elder, K., Marshall, H. P., Vuyovich, C., Kim, E., and Mason, M.: SnowEx Meteorological Station Measurements from Grand Mesa, CO, Version 1, NASA National Snow and Ice Data Center Distributed Active Archive Center, 2022.

Landry, C. C., Buck, K. A., Raleigh, M. S., and Clark, M. P.: Mountain system monitoring at Senator Beck Basin, San Juan Mountains, Colorado: A new integrative data source to develop and evaluate models of snow and hydrologic processes, Water Resour. Res., 50, 1773–1788, https://doi.org/10.1002/2013WR013711, 2014.

Lundquist, J. D. and Lott, F.: Using inexpensive temperature sensors to monitor the duration and heterogeneity of snow-covered areas, Water Resour. Res., 44, https://doi.org/10.1029/2008WR007035, 2008.

https://doi.org/10.5194/egusphere-2024-2249
Preprint. Discussion started: 22 August 2024

Mekonnen, Z. A., Riley, W. J., Berner, L. T., Bouskill, N. J., Torn, M. S., Iwahana, G., Breen, A. L., Myers-Smith, I. H., Criado, M. G., and Liu, Y.: Arctic tundra shrubification: a review of mechanisms and impacts on ecosystem carbon balance, Environ. Res. Lett., 16, 053001, 2021.

Parr, C., Sturm, M., and Larsen, C.: Snowdrift Landscape Patterns: An Arctic Investigation, Water Resour. Res., 56, e2020WR027823, https://doi.org/10.1029/2020WR027823, 2020.

Shirley, I. A., Mekonnen, Z. A., Wainwright, H., Romanovsky, V. E., Grant, R. F., Hubbard, S. S., Riley, W. J., and Dafflon, B.: Near-Surface Hydrology and Soil Properties Drive Heterogeneity in Permafrost Distribution, Vegetation Dynamics, and Carbon Cycling in a Sub-Arctic Watershed, J. Geophys. Res. Biogeosciences, 127, e2022JG006864, https://doi.org/10.1029/2022JG006864, 2022a.

Shirley, I. A., Mekonnen, Z. A., Grant, R. F., Dafflon, B., Hubbard, S. S., and Riley, W. J.: Rapidly changing high-latitude seasonality: implications for the 21st century carbon cycle in Alaska, Environ. Res. Lett., 17, 014032, https://doi.org/10.1088/1748-9326/ac4362, 2022b.

Singhania, A., Glennie, C., Fernandez-Diaz, J., and Hauser, D.: National Center for Airborne Laser Mapping (NCALM) LiDAR and DEM data from two NGEE Arctic Sites, Seward Peninsula, Alaska, Winter 2022, Gener. Ecosyst. Exp. Arct. Data Collect. Oak Ridge Natl. Lab. US Dep. Energy Oak Ridge Tenn. USA, NGA314, https://doi.org/10.5440/1984094, 2023a.

Singhania, A., Glennie, C., Fernandex-Diaz, J., and Hauser, D.: National Center for Airborne Laser Mapping (NCALM) Lidar DEM data from five NGEE Arctic Sites, Seward Peninsula, Alaska, August 2021, Gener. Ecosyst. Exp. Arct. Data Collect. Oak Ridge Natl. Lab. US Dep. Energy Oak Ridge Tenn. USA, NGA270, https://doi.org/10.5440/1832016, 2023b.

Staub, B. and Delaloye, R.: Using Near-Surface Ground Temperature Data to Derive Snow Insulation and Melt Indices for Mountain Permafrost Applications: Snow and Melt Indices Derived from GST Data, Permafr. Periglac. Process., 28, 237–248, https://doi.org/10.1002/ppp.1890, 2017.

Stuefer, S. L., Kane, D. L., and Dean, K. M.: Snow Water Equivalent Measurements in Remote Arctic Alaska Watersheds, Water Resour. Res., 56, e2019WR025621, https://doi.org/10.1029/2019WR025621, 2020.

Sturm, M. and Holmgren, J.: Effects of microtopography on texture, temperature and heat flow in Arctic and sub-Arctic snow, Ann. Glaciol., 19, 63–68, https://doi.org/10.3189/1994AoG19-1-63-68, 1994.

Sulman, B. N., Salmon, V. G., Iversen, C. M., Breen, A. L., Yuan, F., and Thornton, P. E.: Integrating Arctic Plant Functional Types in a Land Surface Model Using Above- and Belowground Field Observations, J. Adv. Model. Earth Syst., 13, e2020MS002396, https://doi.org/10.1029/2020MS002396, 2021.

Tsang, L., Durand, M., Derksen, C., Barros, A.P., Kang, D.H., Lievens, H., Marshall, H.P., Zhu, J., Johnson, J., King, J. and Lemmetyinen, J., 2021. Global monitoring of snow water equivalent using high frequency radar remote sensing. The Cryosphere Discussions, 2021, pp.1-57.

https://doi.org/10.5194/egusphere-2024-2249
Preprint. Discussion started: 22 August 2024

Wang, C., Shirley, I., Wielandt, S., Lamb, J., Uhlemann, S., Breen, A., Busey, R. C., Bolton, W. R., Hubbard, S., and Dafflon, B.: Local-scale heterogeneity of soil thermal dynamics and controlling factors in a discontinuous permafrost region, Environ. Res. Lett., 19, 034030, https://doi.org/10.1088/1748-9326/ad27bb, 2024.

Wieder, W. R., Kennedy, D., Lehner, F., Musselman, K. N., Rodgers, K. B., Rosenbloom, N., Simpson, I. R., and Yamaguchi, R.: Pervasive alterations to snow-dominated ecosystem functions under climate change, Proc. Natl. Acad. Sci. U. S. A., 119, e2202393119, https://doi.org/10.1073/pnas.2202393119, 2022.

Wilcoxon, F.: Individual Comparisons by Ranking Methods, Biom. Bull., 1, 80–83, https://doi.org/10.2307/3001968, 1945.